Comment on "operando DRIFTS and XANES study of deactivating effect of CO2 on a Ce0.8Cu0.2O2 CO-PROX catalyst"

ARTICLE *in* THE JOURNAL OF PHYSICAL CHEMISTRY C · NOVEMBER 2011

Impact Factor: 4.77 · DOI: 10.1021/jp2047773

2 AUTHORS:

Dominique Bazin
Collège de France
286 PUBLICATIONS **3,159** CITATIONS
SEE PROFILE

J. J. Rehr
University of Washington Seattle
410 PUBLICATIONS **18,716** CITATIONS
SEE PROFILE

THE JOURNAL OF PHYSICAL CHEMISTRY C

COMMENT

pubs.acs.org/JPCC

Comment on "Operando DRIFTS and XANES Study of Deactivating Effect of CO_2 on a $Ce_{0.8}Cu_{0.2}O_2$ CO-PROX Catalyst"

D. Bazin*,† and J. J. Rehr‡

†LPS, Bât. 510 D, Université Paris-Sud, 91405 Orsay cedex, France

‡Department of Physics, University of Washington, Seattle, Washington 98195, United States

Currently, there is considerable interest in the development of materials based on nanometer scale metallic clusters for various purposes,[1−4] including catalysis[5−7] and magnetism.[8] Among the different techniques used to characterize their structural characteristics, XAS (X-ray Absorption Spectroscopy), a technique specific to synchrotron radiation, has been extraordinarily successful.[9] This is due to its capacity to describe in situ structural information of materials lacking long-range order, including amorphous and nanometer scale clusters.[10] However, this technique also has some major disadvantages. For example, XAS is unsensitive to polydispersity[11] and quite inefficient to characterize significantly the metallic part of the catalyst to point out stacking defaults.[12]

Different sample environments have been developed to mimic chemical reactions during which the structural investigation through XAS spectroscopy occurs.[13−17] Thanks to the high photon flux of third-generation photon factories, major improvements have been made to reduce significantly the acquisition time.[18] Such improvements include different elements of beamline dedicated to XAS, including monochromators[19−22] and/or detectors.[23−25] While minutes were required to complete an absorption spectrum in the 80s, the acquisition time now has been reduced to some milliseconds, leading to several major breakthroughs in material sciences.[26−28]

Access of X-ray absorption spectra corresponding to the very first steps of the genesis of nanometer scale metallic clusters constitutes an exciting opportunity. When metallic clusters contain very few atoms, we may suppose that the interaction with the support cannot be considered as a perturbation and may influence significantly its structural characteristics. In a previous study,[29] the appearance of long metal−metal distances of the same range order as that of the bond lengths existing in the alumina network has been underlined at the very first step of the genesis of the metallic cluster. Such a dynamic approach can be quite exciting for the investigation of bimetallic systems for which the knowledge of the repartition of the two metals inside the cluster constitutes major structural information.[30−35]

Among the research topics treated in this literature, numerous works have focused on the genesis of nanometer scale metallic clusters or their reactivity.[36−38] Due to their nanometer sizes, particular attention has to be paid to the analysis procedure of the near-edge signal (i.e., the XANES) of such materials. We have previously emphasized that for the nanometer scale metallic cluster of copper[39] the XANES collected at the K-edge is sensitive to both the size and morphology of the cluster. For 5d metals, such as platinum, we have previously studied the relationship between the white line and the size of clusters. We found that two physical effects are responsible for the intensity of the white line: (i) the size of the cluster, which can be considered as an intrinsic effect, since the density of states of a nanometer scale platinum cluster are far from the bulk counterpart, and (ii) a possible charge transfer between the cluster and the support, which can be considered as an extrinsic one.[40] Due to the importance of Pt in catalysis, numerous investigations have been dedicated to the modifications of the white line of Pt nanometer scale clusters.[41−43]

During operando experiments, different statistical methods have been developed to analyze series of spectra collected during the genesis of nanometer scale metallic clusters. Among them, one widely used approach is based on principal component analysis (PCA).[44,45] PCA assumes that the variable (i.e., the absorbance of a set of XANES spectra) can be represented mathematically by a linear combination of independent components alternatively referred to as factors or eigenvectors. Such analysis has been used in several recent investigations at the Fe,[46] Co,[47] Zn,[48] As,[49] Se,[50,51] Mo,[52] Pd,[53] K edge.

The aim of this comment is to show that special attention has to be paid to the choice of these independent components for a quantitative interpretation. More precisely, PCA analysis based on reference compounds such as metal foil for the metallic state is not a reliable approach for the analysis of nanometer scale metallic particles. Of note, not all PCA analyses dismiss particle size/shape effects on XANES. To show this, we have performed a set of numerical simulations of the XANES signal at the K- and L-edges of 3d, 4d, and 5d transition metals. For each case, we consider a nanometer scale metallic cluster of 13 atoms and compare it with a numerical simulation of the corresponding metallic foil. Thus full multiple scattering calculations (see ref 54 for a recent review) in real space have been performed by using the ab initio real-space multiple-scattering XAS code FEFF9. As discussed previously, the XAFS oscillations in FEFF9 are expressed as a sum of independent multiple scattering contributions. Each such contribution can be expressed as

$$\chi^n(k) = \chi_0^n(k)\,\exp(-L_n/\lambda n - 2k^2\sigma_n^2)$$

$$\chi_0^n(k) = F_n(k)\,\sin(kL_n + \theta_n(k))$$

Here, n represents a single or multiple scattering paths and L_n is the total path length. F_n and θ_n are the effective scattering amplitude and phase shift which depend on k and on the specifics of the scattering path involved such as the atomic potential parameters.

Received: May 23, 2011
Revised: September 13, 2011
Published: September 14, 2011

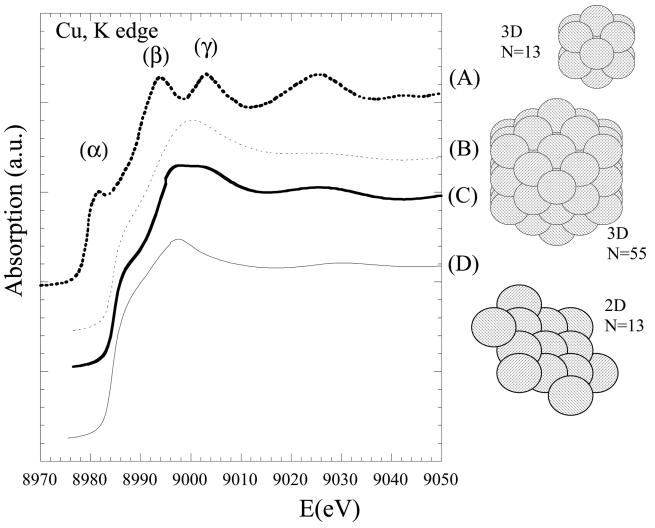

Figure 1. FEFF9 simulations performed at the Cu K edge for the metallic foil (A), for a 3D cuboctahedral 13 atom cluster (B), for a 3D cuboctahedral 55 atom cluster (B), and for a 2D 13 atoms cluster (D).

In Figure 1, a set of numerical simulations are reported where the XANES of a metallic foil is compared to numerical simulations on a 13 atom cluster. As already mentioned, the cluster size constitutes a significant structural parameter for Cu. These numerical calculations show that the choice of the copper metallic foil is definitely not valid for Cu^0.[55] At this point, we stress that such a size effect is only significant for small clusters, e.g., those containing an order of 10−50 atoms. For clusters containing more atoms, such effects become negligible.

Numerical simulations performed with FEFF9 indicate that it is not possible to take into account the loss of the $\beta-\gamma$ structures, which corresponds to cuboctahedral 13 or 55 atom clusters with a PCA analysis in which this structure exists, the reference spectra for the PCA simulation coming or not from experimental data (Figure 7 right, ref 55). While the left and the right parts of Figure 6 of ref 55 are correct, the point where the Cu^0 state begins to exist is probably not at 225 °C.

Such information does not change the final conclusion of the paper from a catalytic point of view but clearly shows that it is important to correlate the XANES measurements and the structural parameters obtained through EXAFS spectroscopy to perform a significant PCA simulation. That is, if the number of metallic number around Cu atoms is high, the metallic foil component can be selected for Cu^0. If the number of metallic number around Cu atoms is low, particular attention has to be paid to the simulation. Note that even for quite large clusters a relaxation process may exist,[56] and the effect of the interatomic distance on the XANES can also be significant.

Similar arguments can be used for Pt (Figure 2) and Au clusters (Figure 3). If we consider now a L_{III} edge, significant effects on the intensity of the white line exist only for 13 or 55 atom clusters. We have already discussed the case of Pt in detail previously. The case of Au is quite interesting because the reducibility of gold of nanometer scale metallic particle has been widely studied,[57−59] and the size effect of the XANES on the L edges is rarely discussed. While the acquisition time is reduced through the recent technological developments, particular attention has to be paid to the data analysis related to following kinetics of the reduction process.

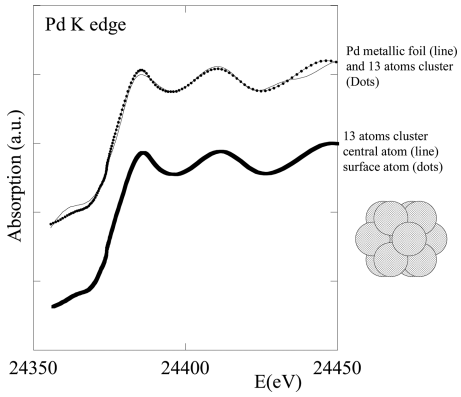

Figure 2. FEFF9 simulations performed at the Pd K edge for the metallic foil (upper part in line) and for the 13 atom cuboctahedral cluster (upper part in dots). To plot the simulations of the 13 atom cuboctahedral cluster, an average has been done between the contribution of the central atoms (lower part in line) and of the surface atoms (lower part in dots).

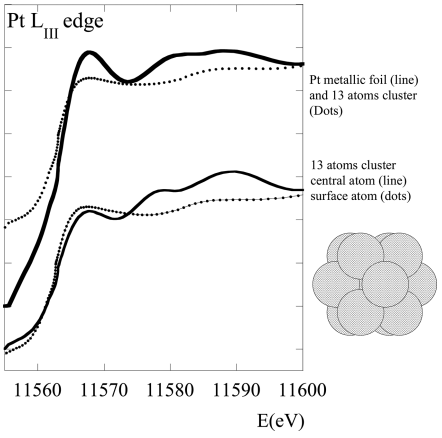

Figure 3. FEFF simulations performed at the Pt L_{III} edge for the metallic foil (upper part in line) and for the cuboctahedral 13 atom cluster (upper part in dots). To plot the simulations of the 13 atom cluster, an average has been done between the contribution of the central atoms (lower part in line) and of the surface atoms (lower part in dots).

The case of palladium (Figure 4) is also quite interesting, this element being extensively studied in heterogeneous catalysis.[60] Remarkably, the difference between the Pd foil and 13 atom clusters is quite small. As noticed by Hayashi et al., XANES features are, however, often smeared out because of the natural broadening that originates from the finite core-hole lifetime.[61] More precisely, the broadening increases with increasing atomic number (Z) and for the K shell ranges from 0.86 eV (Sc, $Z = 21$) to 40 eV (W, $Z = 74$).[62] Thus, the lifetime of the core-hole leads to a significant broadening and thus to a disappearance of the different features present at the Pd edge. Again, these arguments are valid for other 4d metals such as rhodium. Such an argument based on the variation of the core-hole lifetime with atomic number leads to the fact that for soft X-ray absorption spectroscopy, i.e., L edges of 3d transition metals, the lack of long-range order affects also the edge part. Indeed, at the Co $L_{II,III}$ edges, disappearance of the different features associated with Co^{2+} O_h

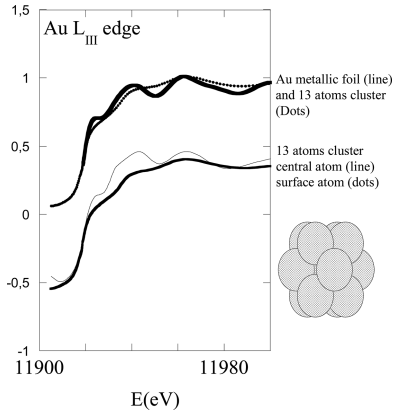

Figure 4. FEFF simulations performed at the Au L_{III} edge for the metallic foil (upper part in line) and for the 13 atom cluster (upper part in dots). To plot the simulations of the 13 atom cluster, an average has been done between the contribution of the central atom (lower part in line) and of the surface atoms (lower part in dots).

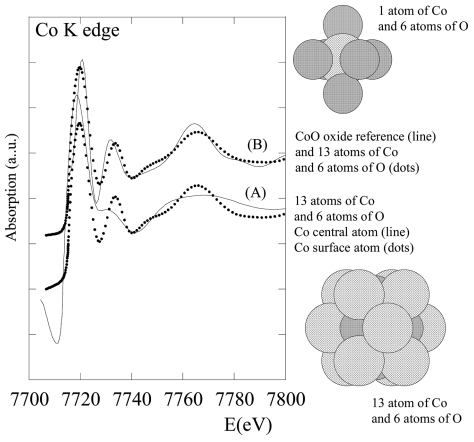

Figure 5. FEFF simulations performed at the CoK edge for the CoO (upper part in line) and for the Co cluster (upper part in dots). To plot the simulations of the CoO cluster, an average has been carried out for the contribution of the central atom (lower part in line) and of the surface atoms (lower part in dots).

symmetry have been measured, and the hypothesis of disorder in the first coordination sphere of the cobalt atoms has been proposed.[63]

Moreover, particular attention has to be paid to the data analysis related to following kinetics of the reduction processes. We would thus like to underline the fact that such a size effect on the XANES part exists for oxide compounds as well as for sulfur compounds.

To assess the case of oxide materials, numerical simulations have been performed regarding CoO oxide (Figure 5). First, we have plotted the contributions of the central and the surface atoms of a cluster of CoO containing 13 atoms of Co atoms (1 Co central atom and 12 Co surface atoms) and 6 atoms of O atoms (Figure 5, (A)). As expected for nanometer scale materials, we are far from the stoichiometry. Second, if we compare the simulation obtained for CoO bulk and the 13Co6O cluster, we can see a significant difference in line with what we have observed for the metallic phase.

CONCLUSION

With the emergence of a third generation of photon factories, the reduction of the acquisition time offers the opportunity to gather information regarding the initial steps in the genesis of nanometer scale metallic clusters. For such applications, special attention has to be paid to the analysis procedure, taking into account that significant size and morphology effects exist in the XANES part of an X-ray absorption spectrum.

Through numerical simulations based for example on the real-space FEFF code, we can assess these effects and thus elucidate both the advantages and limitations of the PCA analysis procedures. Of note, such an approach is relevant for metallic and nonmetallic nanometer scale entities. During a reduction process (respectively, for a sulfurization process), size effect on the XANES (as well as a possible coming from relaxation/heterometallic bonds/morphology) has to be introduced in the PCA simulation for both metallic and oxide compounds (respectively, sulfur compounds).

As a conclusion, further calculations are required to obtain a precise description of structural modification of nanometer scale material, and a XANES analysis through FEFF9−PCA, which has to integrate data coming from other techniques such as EXAFS, RAMAN, or scattering techniques[64] as well as ab initio calculations of the electronic structures based for example on a tight-binding model, remains to be more deeply addressed.

REFERENCES

(1) Friedel, J. *Physics of Metals*; Cambridge University Press: Cambridge, 1978; Vol. 1.
(2) Somorjai, G. A. *Principles of surface chemistry and catalysis*; Wiley: New York, 1994.
(3) El-Sayed, M. A. *Acc. Chem. Res.* **2001**, *34*, 257–264.
(4) Zhou, B. ; Hermans, S. ; Somorjai, G. A. *Nanotechnology in catalysis*; Springer Verlag: Berlin, 2004.
(5) Balcha, T.; Strobl, J. R.; Fowler, C.; Dash, P.; Scott, R. W. J. *ACS Catal.* **2011**, *1*, 425–436.
(6) Bazin, D.; Lynch, J.; Ramos-Fernandez, M. *Oil Gas Sci. Technol.* **2003**, *58*, 667–683.
(7) Marx, S.; Krumeich, F.; Baiker, A. *J. Phys. Chem. C* **2011**, *115* 8195–8205.
(8) Figueroa, S. J. A.; Stewart, S. J.; Rueda, T.; Hernando, A.; de la Presa P. *J. Phys. Chem. C* **2011**.
(9) Sayers, D. E.; Lytle, F. W.; Stern, E. A. *Adv. X-ray Anal.* **1970**, *13* 248.
(10) Revel, R.; Bazin, D.; Elkaim, E.; Kihn, Y.; Dexpert, H. *J. Phys. Chem. B* **2000**, *104*, 9828–9835.
(11) Moonen, J.; Slot, J.; Lefferts, L.; Bazin, D.; Dexpert, H. *Phys. B* **1995**, *208*, 689–690.
(12) Ducreux, O.; Rebours, B.; Lynch, J.; Roy-Auberger, M.; Bazin, D. *Oil Gas Sci. Technol. − Rev. IFP* **2009**, *64*, 49–62.
(13) Hannemann, S.; Casapu, M.; Grunwaldt, J.-D.; Haider, P.; Trüssel, P.; Baiker, A.; Welter, E. *J. Synchrotron Radiat.* **2007**, *14* 345–354.
(14) Pettiti, I.; Gazzoli, D.; Inversi, M.; Valigi, M.; De Rossi, S.; Ferraris, G.; Porta, P.; Colonna, S. *J. Synchrotron Radiat.* **1999**, *6*, 1120–1124.
(15) Guilera, G.; Gorges, B.; Pascarelli, S.; Vitoux, H.; Newton, M. A.; Prestipino, C.; Nagai, Y.; Hara, N. *J. Synchrotron Radiat.* **2009**, *16* 628–634.
(16) Girardon, J.-S.; Khodakov, A. Y.; Capron, M.; Cristol, S.; Dujardin, C.; Dhainaut, F.; Nikitenko, S.; Meneau, F.; Bras, W.; Payen, E. *J. Synchrotron Radiat.* **2005**, *12*, 680–684.
(17) Berry, A. J.; Shelley, J. M. G.; Foran, G. J.; O'Neill, H. S. C.; Scott, D. R. *J. Synchrotron Radiat.* **2003**, *10*, 332–336.

(18) Newton, M. A.; Dent, A. J.; Evans *J. Chem. Soc. Rev.* **2002**, *31* 83–95.
(19) Sayers, D.; Cantrell, J.; Bazin, D.; Dexpert, H.; Fontaine, A.; Lagarde, P.; Lynch, J.; Bournonville, J. P. *Phys. B: Condens. Matter* **1989**, *158*, 206–207.
(20) Frahm, R. *NIM A* **1988**, *270*, 578–581.
(21) Stötzel, J.; Lützenkirchen-Hecht, D.; Frahm, R. *J. Synchrotron Radiat.* **2011**, *18*, 165–175.
(22) Stötzel, J.; Lützenkirchen-Hecht, D.; Fonda, E.; De Oliveira, N.; Briois, V.; Frahm, R. *Rev. Sci. Instrum.* **2008**, *79*, 83–107.
(23) Okumura, K.; Yoshino, K.; Kato, K.; Niwa, N. *J. Phys. Chem. B* **2005**, *109*, 12380–12386.
(24) Dent, A. J. *Top. Catal.* **2002**, *18*, 27–35.
(25) Bauer, M.; Heusel, G.; Mangold, S.; Bertagnolli, H. *J. Synchrotron Radiat.* **2010**, *17*, 273–279.
(26) Newton, M. A.; Dent, A. J.; Fiddy, S. G.; Jyoti, B.; Evans, J. *Catal. Today* **2007**, *126*, 64–72.
(27) Reimann, S.; Stötzel, J.; Frahm, R.; Kleist, W.; Grunwaldt, J. D.; Baiker, A. *J. Am. Chem. Soc.* **2011**, *133*, 3921–3930.
(28) Föttinger, K.; van Bokhoven, J. A.; Nachtegaal, M.; Rupprechter, G. *J. Phys. Chem. Lett.* **2011**, *2*, 428–433.
(29) Bazin, D.; Dexpert, H.; Bournonville, J. P.; Lynch, J. *J. Catal.* **1990**, *123*, 86–97.
(30) Barcaro, G.; Fortunelli, A.; Polak, M.; Rubinovich, L. *Nano Lett.* **2011**, *11*, 1766–1769.
(31) Small, M. W.; Sanchez, S. I.; Menard, L. D.; Kang, J. H.; Frenkel, A. I.; Nuzzo, R. G. *J. Am. Chem. Soc.* **2011**, *133*, 3582–3591.
(32) Chou, H. L.; Lai, F. J.; Su, W. N.; Pillai, K. C.; Sarma, L. S.; Hwang, B. J. *Langmuir* **2011**, *27*, 1131–1135.
(33) Wang, X.; Li, N.; Pfefferle, L. D.; Haller, G. L. *J. Phys. Chem. C* **2010**, *114*, 16996–17002.
(34) Hugon, A.; Delannoy, L.; Krafft, J. M.; Louis, C. *J. Phys. Chem. C* **2010**, *114*, 10823–10835.
(35) Bazin, D.; Dexpert, H.; Lynch, J.; Bournonville, J. P. *J. Synchrotron Radiat.* **1999**, *6*, 465–469.
(36) Schneider, S.; Bazin, D.; Garin, F.; Maire, G.; Capelle, M.; Meunier, G.; Noirot, R. *Appl. Catal. A* **1999**, *189*, 139–145.
(37) Bideberripe, H. P.; Ramallo-López, J. M.; Figueroa, S. J. A.; Jaworski, M. A.; Casella, M. L.; Siri, G. J. *Catal. Commun.* **2011**, *12* 1280–1285.
(38) Cónsul, J. M. D.; Baibich, I. M.; Martins Alves, M. C. *Catal. Commun.* **2011**, *12*, 1357–1360.
(39) Bazin, D.; Rehr, J. J. *J. Phys. Chem. B* **2003**, *107*, 12398–12402.
(40) Bazin, D.; Sayers, D.; Rehr, J. J.; Mottet, C. *J. Phys. Chem. B* **1997**, *101*, 5332–5336.
(41) Lei, Y.; Jelic, J.; Nitsche, L. C.; Meyer, R.; Miller, J. *Topics Catal.* **2011**, *54*, 334–348.
(42) Becker, E.; Carlsson, P. A.; Kylhammar, L.; Newton, M. A.; Skoglundh, M. *J. Phys. Chem. C* **2011**, *115*, 944–951.
(43) Bus, E.; van Bokhoven, J. A. *J. Phys. Chem. C* **2007**, *111* 9761–9768.
(44) Malinowski, E. R. *Factor Analysis in Chemistry*, 2nd ed.; Wiley: New York, 1991.
(45) Fernandez-Garcıa, M. *Catal. Rev. Sci. Eng.* **2002**, *44*, 59–75.
(46) Piovano, A.; Agostini, G.; Frenkel, A. I.; Bertier, T.; Prestipino, C.; Ceretti, M.; Paulus, W.; Lamberti, C. *J. Phys. Chem. C* **2011**, *115* 1311–1322.
(47) Rochet, A.; Moizana, V.; Pichon, Ch.; Diehl, F.; Berliet, A.; Briois, V. *Cat. Today* **2011**.
(48) McPeak, K. M.; Becker, M. A.; Britton, N. G.; Majidi, N.; Bunker, B. A.; Baxter, J. B. *Chem. Mater.* **2010**, *22*, 6162–6170.
(49) Planer-Friedrich, B.; Suess, E.; Scheinost, A. C.; Wallschläger, D. *Anal. Chem.* **2010**, *82*, 10228–10235.
(50) Weekley, C. A.; Aitken, J. B.; Vogt, S.; Finney, L. A.; Paterson, D. J.; de Jonge, M. D.; Howard, D. L.; Musgrave, I. F.; Harris, H. H. *Biochemistry* **2011**, *50*, 1641–1650.
(51) Lenz, M.; van Hullebusch, E. D.; Farges, F.; Nikitenko, S.; Corvini, P. F. X.; Lens, P. N. L. *Environ. Sci. Technol.* **2011**, *45*, 1067–1073.
(52) Essilfie-Dughan, J.; Pickering, I. J.; Hendry, M. J.; George, G. N.; Kotzer, T. *Environ. Sci. Technol.* **2011**, *45*, 455–460.
(53) Iglesias-Juez, A.; Kubacka, A.; Fernandez-García, M.; Di Michiel, M.; Newton, M. A. *J. Am. Chem. Soc.* **2011**, *133*, 4484–4489.
(54) Rehr, J. J.; Kas, J. J.; Prange, M. P.; Sorini, A. P.; Takimoto, Y.; Vila, F. *C. R. Phys.* **2009**, *10*, 548–559.
(55) Gamarra, D.; Fernandez-Garcıa, M.; Belver, C.; Martinez-Arias, A. *J. Phys. Chem. C* **2010**, *114*, 18576–18582.
(56) Mottet, C.; Tréglia, G.; Legrand, B. *Surf. Sci.* **1997**, *383* L719–L727.
(57) Sandoval, A.; Aguilar, A.; Louis, C.; Traverse, A.; Zanella, R. *J. Catal.* **2011**, *281*, 40–49.
(58) Ohyama, J.; Teramura, K.; Shishido, T.; Hitomi, Y.; Kato, K.; Tanida, H.; Uruga, T.; Tanaka, T. *Chem. Phys. Lett.* **2011**, *507*, 105–110.
(59) Fang, Y. L.; Miller, J. T.; Guo, N.; Heck, K. N.; Alvarez, P. J. J.; Wong, M. S. *Catal. Today* **2011**, *160*, 96–102.
(60) Grunwaldt, J. D.; Maciejewski, M.; Baiker, A. *Phys. Chem. Chem. Phys.* **2003**, *5*, 1481–1488.
(61) Hayashi, H.; Udagawaa, Y.; Caliebe, W. A.; Kao, C. C. *Chem. Phys. Lett.* **2003**, *371*, 125–130.
(62) Krause, O.; Oliver, J. H. *J. Phys. Chem. Ref. Data* **1979**, *8* 329–379.
(63) Bazin, D.; Kovacs, I.; Guczi, L.; Parent, P.; Laffon, C.; De Groot, F.; Ducreux, O.; Lynch, J. *J. Catal.* **2000**, *189*, 456–462.
(64) Bazin, D.; Guczi, L.; Lynch, J. *Appl. Catal.* **2002**, *226*, 87–113.